Applied Clay Science 171 (2019) 1–5

Contents lists available at ScienceDirect

Applied Clay Science

journal homepage: www.elsevier.com/locate/clay

Note

Facile sample preparation method allowing TEM characterization of the stacking structures and interlayer spaces of clay minerals

Dong Liu[a,b], Qian Tian[a,b], Peng Yuan[a,b,*], Peixin Du[a], Junming Zhou[a,b], Yun Li[a,b], Hongling Bu[a], Jieyu Zhou[a,b]

[a] CAS Key Laboratory of Mineralogy and Metallogeny/Guangdong Provincial Key Laboratory of Mineral Physics and Materials, Guangzhou Institute of Geochemistry, Institutions of Earth Science, Chinese Academy of Sciences, Guangzhou 510640, China
[b] University of Chinese Academy of Sciences, Beijing 100049, China

ARTICLE INFO

Keywords:
Sample preparation
TEM
Clay minerals
Stacking structure
Interlayer organic matter

ABSTRACT

Transmission electron microscopy (TEM) is an essential and irreplaceable technique for studying the micromorphology and microstructure of clay minerals. However, observing layer stacking and detecting the interlayer spaces of clay minerals by TEM are still major challenges, due to the difficulty of finding suitable fields of view for clay planes along the [00*l*] direction. A simple and effective sample pretreatment method was proposed here for TEM characterization of clay mineral stacking structures and interlayer spaces. Using this method, clay mineral-bearing ultrathin slices, in which clay minerals particles showed an orientated arrangement, were prepared based on the resin embedding method. The (00*l*) plane of clay minerals was exposed toward electron beams during TEM analysis, and fields of view along the [00*l*] direction were observed, accordingly. This method is thus particularly useful for the observation of stacking information and detection of interlayer regions in clay minerals. The validity of this method is exemplified by its application to pure kaolinite and clay mineral-rich shale samples which contains several clay minerals and the clay mineral-organic matter complexes.

1. Introduction

Transmission electron microscopy (TEM) is a powerful technique for clay mineral analysis and has been widely used for more than half a century (Brown and Rich, 1968; Wenk, 1976; Marcks et al., 1989; Clinard et al., 2003). TEM enables direct observation of the micromorphology and microstructure of clay minerals. In particular, high-resolution (HR) TEM with an X-ray diffraction (XRD) spectrometer can provide abundant information on unique microstructural characteristics of clay minerals, such as interstratification, mixed layer structures, atomic arrangements, and crystal defects (Brown and Rich, 1968; Marcks et al., 1989; Leapman and Hunt, 1991; Murakami et al., 1999; Kogure et al., 2001, 2002; Clinard et al., 2003; Chen et al., 2004; Chen and Wang, 2007a, 2007b; Hong et al., 2014).

The stacking structure is one of the most important structural characteristics of clay minerals, and HRTEM observation of stacking provides plentiful information of clay minerals, such as polytypes and stacking faults (Gareth and Goringe, 1979; Kogure and Banfield, 1998; Kogure et al., 2001, 2002). Moreover, the interlayer structure of many types of clay minerals (such as swelling clay minerals) is very important, because the characteristics of the interlayer structure are highly relevant to the reactivity of the clay minerals. For example, the interlayer distance of clay minerals strongly affects the porosity of clay minerals and is closely related to the adsorptive properties of clay minerals. (Yuan et al., 2008; Brigatti et al., 2013). In addition, the interlayer region of clay minerals is an important place for hosting guest molecules such as metal cations or organic matter (OM), which are highly relevant to some key geological processes, including hydrocarbon generation driven by clay minerals and to the development of novel clay-based materials (Xi et al., 2005; Theng, 2012, 2018; Wu et al., 2012; Zhang et al., 2012; Liu et al., 2013b; Yuan et al., 2013; Lv et al., 2015; Jiang et al., 2016; Bu et al., 2017). Gas molecule adsorption in the interlayer space of clay minerals has also been demonstrated (Liu et al., 2013a).

TEM characterization of the stacking structure or interlayer structure of clay minerals is highly desirable for all of the abovementioned properties or applications of clay minerals. However, HRTEM observation for layer stacking and the interlayer space of clay minerals is still a challenge. Normally, views of layer arrangement observed by TEM are (*hk*0) planes of clay minerals rather than (00*l*) planes, due to the random arrangement of clay mineral particles when using conventional powder deposit or resin embedding methods (Wenk, 1976;

* Corresponding author at: Guangzhou Institute of Geochemistry, Institutions of Earth Science, Chinese Academy of Sciences, Wushan, Guangzhou 510640, China.
E-mail address: yuanpeng@gig.ac.cn (P. Yuan).

https://doi.org/10.1016/j.clay.2019.01.019
Received 13 December 2018; Received in revised form 23 January 2019; Accepted 27 January 2019

Iijima and Buseck, 1978; Kogure et al., 2006, 2011). Therefore, looking for a suitable particle that occasionally shows the (00*l*) planes parallel to the incident direction of electron beams is usually time-consuming.

Furthermore, clay minerals have very low electron-beam-resistance (Kogure, 2013). Damage and even deconstruction of the local structure of clay minerals readily occur by knock-on damage and/or radiolytic damage as the sample undergoes electron beam radiation (Clinard et al., 2003; Kogure et al., 2006, 2011; Lutterotti et al., 2010). Therefore, slow operation easily misses the chance to record images because of the damage resulting from electron beams (Drits et al., 2012). The strategy commonly adopted to avoid or reduce the damage induced by the electron beam is shortening the time for observing suitable views. This strategy can decrease the exposing time of clay minerals under irradiation. However, as mentioned above, quickly finding the suitable views along the [*hk*0] direction of clay minerals is very difficult based on the preparation of HRTEM samples. To solve this problem, a sample pretreatment method allowing rapid location of the target views of the stacking structure is needed.

In this work, a novel resin embedding method for TEM sample preparation was proposed. This method significantly increases the probability of observing the (00*l*) planes and lowers the difficulty of detecting the layer stacking and interlayer space of clay minerals. The unique property of preferred orientation of clay minerals is utilized in the method, whereby a thin clay mineral-film with an orientated arrangement is tiled between two prepared solidified resin pieces. Kaolinite and the clay minerals in clay-rich shale samples were selected as models for evaluating the applicability of the sample preparation method to pure clay minerals and clay-rich rocks.

2. Materials and methods

2.1. Kaolinite and shale samples

A high-purity kaolinite (denoted Kaol) sample, obtained from Maoming in Guangdong Province, China, was used as received without further purification. The chemical composition (wt%) of kaolinite was as follows: SiO_2, 46.75; Al_2O_3, 39.15; Fe_2O_3, 1.02; MgO, 0.10; CaO, 0.21; K_2O, 0.25; Na_2O, 0.26; MnO, 0.01; TiO_2, 0.32; P_2O_5, 0.04; and loss on ignition, 11.92.

Raw shale samples collected from the Yanchang shale area in the Ordos Basin, north-central China were selected as a model to evaluate the TEM preparation method. The Yanchang shale area is one of the most important petroleum resources in China. (Zhang et al., 2007; Guo et al., 2014). The shale samples obtained in this study have high total organic carbon contents (2.02 wt%) and several minerals, mainly including kaolinite, montmorillonite, illite, illite-smectite mixed-layer mineral, and quartz.

2.2. Preparation of samples for TEM characterization

A plastic mold with a size of 5.0 × 2.0 × 1.0 cm was used as a holder, and Spur resin (SPI Supplies, Shanghai, China) was injected until half the volume of the mold was reached. Solidification of the resin-containing mold was performed in an electric oven at 70 °C for 15 h.

Kaolinite or shale samples were ground before treatment. Gravitational settling in a column of water was then used to obtain particles with sizes < 2 μm for the HRTEM analysis. A dispersion was prepared by mixing 10.0 mg of particles with 1.0 mL of water. An ultrasonic process was then carried out in order to disperse the minerals well. The dispersion was dropped onto the abovementioned solidified resin slide to form a thin film of clay minerals (with thickness of 1 mg/1 cm^2) through sedimentation. After the dispersion was air-dried, Spur resin was injected into the mold again and then solidified. The solidified samples were cut along the smallest plane and vertically to the largest plane with a diamond knife (Microstar Standard) using the Leica EM UC7 Ultramicrotome. Ultrathin sections with thicknesses of 50–80 nm were placed on copper grids without carbon film coating for TEM characterization, whereby the (00*l*) planes of clay particles were preferentially oriented parallel to the incident direction of electron beams (Fig. 1).

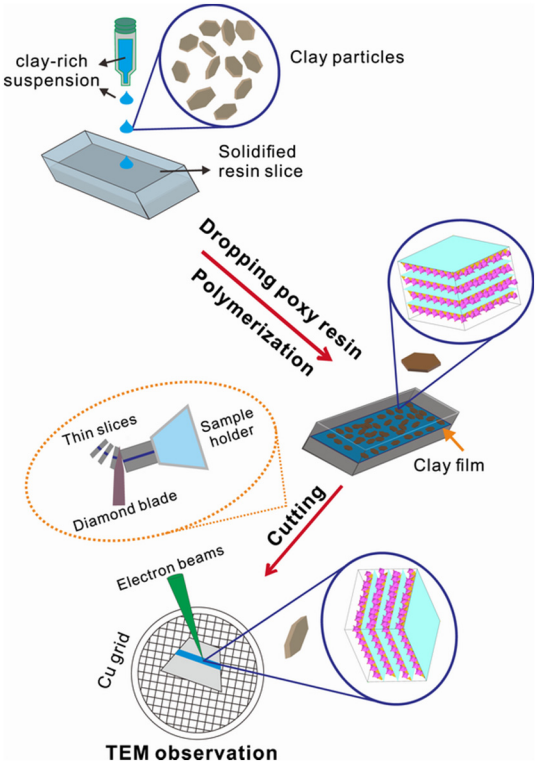

Fig. 1. Schematic representation of the steps for preparation of TEM samples.

2.3. TEM analysis

HRTEM analysis was performed using an FEI Talos F200S field-emission transmission electron microscope with an accelerating voltage of 200 kV. The high-resolution electron energy loss spectroscopy (EELS) study was performed using Gatan Quantum EELS accessory with voltage of 200 kV. Line scans were recorded by the electron beams with steps of 0.5 nm.

3. Results and discussion

Several views of ultrathin sections of kaolinite and shale samples were selected and observed by TEM to exemplify and to show the validity of the sample pretreatment for observing the stacking structure of clay minerals (Fig. 2 for kaolinite and Fig. 3 for shale). Moreover, HRTEM observations combined with EELS analysis were performed to assess the feasibility of this pretreatment method for the detection of OM in interlayer space.

3.1. HRTEM observation for Kaol

For the Kaol sample, many stacking views of kaolinite layers can be observed in one randomly selected region (4.7 × 3.2 μm) of the ultrathin section (Fig. 2a). The presence of such suitable views indicates that finding the views along the [*hk*0] direction of clay minerals using the proposed sample preparation method is easy. Consequently, observation can be rapidly performed, which significantly decreases the electron beam damage during TEM analysis.

Two randomly selected domains in the view of the ultrathin section

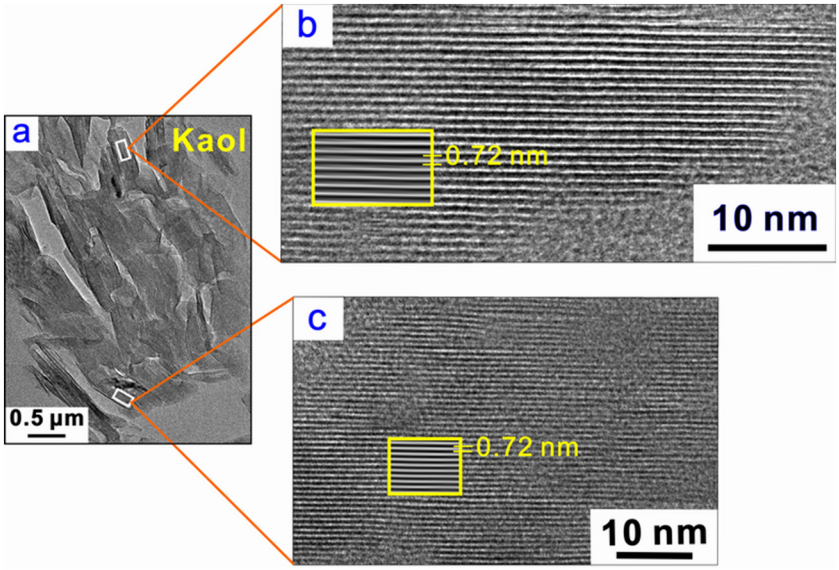

Fig. 2. (a) A TEM image of ultrathin section of Kaol; (b) and (c) HRTEM images of selected domains of (a) further magnified, and the corresponding inverse fast Fourier transforms (IFFT) images (in rectangles of (b) and (c)). Dark and bright stripes represent the layers and the interlayer spaces, respectively.

were selected to investigate the layer stacking information of Kaol (Fig. 2b and c). Dark stripes and bright stripes appear alternately and represent the layers and the interlayer spaces, respectively. IFFT was conducted and more distinct images are displayed (yellow rectangles in Fig. 2b and c). The distance between two adjacent dark stripes is 0.72 nm which agrees well with the ideal basal spacing of kaolinite (Brigatti et al., 2013). The stacking micromorphology characteristics of Kaol corresponded to the well-ordered arrangement of kaolinite layers along or nearly along to the *c*-axis. These results show the high efficiency of the preparation method for TEM observation of kaolinite stacking structures.

3.2. TEM observation for clay minerals in shale samples

Fig. 3a and c display two typical TEM images of ultrathin sections of the shale sample. Similarly, a randomly-selected domain is magnified to observe the stacking information of clay minerals, showing abundant views of layer stacking (Fig. 3b). This result demonstrates that our method is also appropriate for preparing the natural clay-bearing shale samples for TEM observation of clay mineral stacking structures.

Based on the interlayer distances in the one-dimensional lattice fringe, kaolinite (Kaol, ~0.72 nm), illite (I, ~1.0 nm), and illite-smectite (I–Sm, ~2.3 nm) mixed-layer minerals are clearly identified (Fig. 3b1–b3) (Brigatti et al., 2013). Some layer stacking information about these clay minerals is obtained; for example, the I–Sm mixed-layer mineral composed of two illite layers with a smectite layer between them shows a layer unit of ~2.3 nm.

Fig. 3d presents a near atomic-resolution image of the layer stacking of kaolinite in the shale sample, which is identified by the interlayer distance of 0.72 nm. The kaolinite particle displays a basic stacking sequence with a well-crystallized structure, showing that dark spots and bright spots are alternately present. A clearer image (the area marked

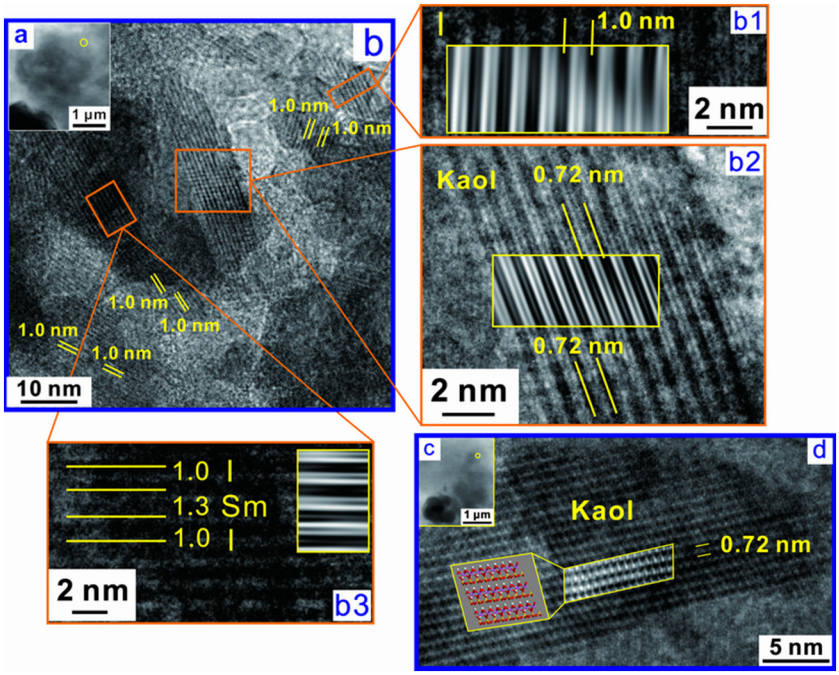

Fig. 3. (a) TEM image of an ultrathin section of a shale sample; (b) HRTEM images of one selected domain of (a) (marked by the yellow circle) further magnified; (b1-b3) HRTEM images of selected domains of (b) and the corresponding IFFT images (in yellow rectangles; dark and bright stripes represent the layers and the interlayer spaces, respectively); (c) Another TEM image of an ultrathin section of shale samples; (d) A HRTEM image of a selected domain of (c) (marked by the yellow circle) further magnified and IFFT images of the selected areas (in yellow parallelogram) with the corresponding simulated crystal structure of illite. (For interpretation of the references to colour in this figure legend, the reader is referred to the web version of this article.)

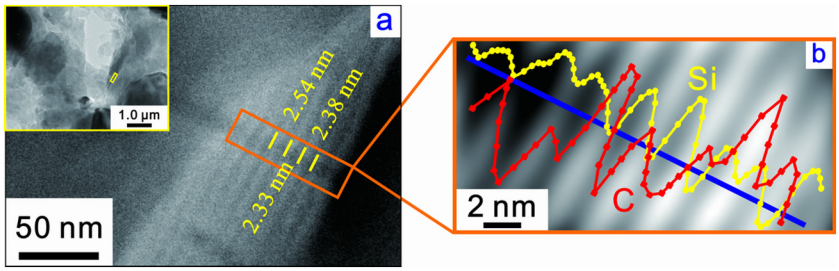

Fig. 4. (a) A HRTEM image of montmorillonite from the selected domain in the ultrathin section (in yellow rectangle, inset of (a)) of the shale sample; (b) IFFT image with magnification of the selected area showing elemental distributions of Si (yellow line) and C (red line). Dark and bright stripes represent the layers and the interlayer spaces, respectively. (For interpretation of the references to colour in this figure legend, the reader is referred to the web version of this article.)

by a parallelogram in Fig. 3d) is obtained after IFFT analysis. The image displays the ordered layer stacking, and no evident stacking faults and crystallized defects are present. This result indicates that the method is also beneficial for observing the atomic arrangements of clay mineral structures.

These results show that the simple preparation process makes locating the layer stacking of various clay minerals along the *c*-axis in natural shale samples easy. The method is effective for HRTEM observations of the stacking micromorphology of clay minerals and of the polytypes and even atomic arrangements of the layer units.

3.3. TEM analysis for interlayer OM of clay minerals in the shale sample

Complexes of clay minerals and OM occur widely in soil and in source rocks, and the interlayer space of clay minerals is believed to be the main storage region of OM (Theng, 2012; Liu et al., 2013b; Yuan et al., 2013). Direct detection of the OM existing in the interlayer space is important not only for identifying OM occurrence but also for evaluating the complexation properties of the OM-clay complex. However, few reports refer to the analysis of interlayer OM using TEM. This lack is mainly due to difficulty of determining the anticipated fields of view of layer stacking.

Shale samples collected in this study possess high OM contents and may contain OM-clay complexes. Thus, the detection of interlayer OM in shale samples based on the pretreatment method confirm the feasibility of HRTEM analysis for interlayer matter of clay minerals and ascertain the interlayer OM occurrence in clay minerals in such shale.

The results indicate that, using the proposed sample preparation method, TEM detection of the interlayer OM is easy. Fig. 4a and b display an HRTEM image of montmorillonite from the selected domain of the ultrathin section of the shale sample and an IFFT images of a magnified selected area, respectively. EELS was used here due to its higher sensitivity for C detection (Leapman and Hunt, 1991). A single montmorillonite particle appears in a selected field of view (inset Fig. 4a). The one-dimensional lattice fringe image of montmorillonite shows clear stacking information of montmorillonite along the [00*l*] direction with basal spacing of > 2.0 nm (Fig. 4a). Performing the high-resolution IFFT, layers (dark stripes) and interlayers spaces (bright stripes) are more clearly distinguished (Fig. 4b). Based on the EELS analysis of the selected domain, the elemental distribution of Si (yellow lines in Fig. 4b) is shown, which corresponds to montmorillonite layers (dark stripes), which indicates the attribution of Si to the Si−O tetrahedral; meanwhile, C (red lines) appears accompanied with bright stripes (Fig. 4b) and is attributed to OM because no other carbon source exists on copper grids without carbon film coating. This result demonstrates the applicability of the proposed method for revealing the existence of interlayer OM in OM-rich shale samples.

4. Conclusions

In this study, a novel sample preparation method is developed for TEM observation/analysis of clay minerals for their stacking structures. A thin clay mineral-film with an orientated arrangement of clay mineral particles was tiled between two solidified resin pieces. Then ultrathin slices for TEM observation were obtained after cutting and loading on the copper grid, whereby views of layer arrangement of clay minerals along the *c*-axis are easily observed. Using this method, layer stacking information of various natural clay minerals can be rapidly obtained. Identification of the types and/or polytypes of clay minerals and of stacking faults in clay minerals could benefit from the proposed method. Moreover, detection of the interlayer organic matter in clay minerals by TEM combined with elemental analysis is simple based on the pretreatment method. Therefore, this TEM sample pretreatment method is promising and could be widely used for the studies on the stacking microstructures and the interlayer spaces of clay minerals.

Acknowledgements

This work was financially supported by the National Natural Science Foundation of China (Grant Nos. 41472044, 41272059 and 41802039), Youth Innovation Promotion Association CAS for the excellent members (2016-81-01), Science Foundation of Guangdong Province, China (Grant No. 2014A030313682), and China Postdoctoral Science Foundation (Grant No. 2018 M633173). This is a contribution (IS-2649) from GIGCAS.

Appendix A. Supplementary data

Supplementary data to this article can be found online at https://doi.org/10.1016/j.clay.2019.01.019.

References

Brigatti, M.F., Galan, E., Theng, B.K.G., 2013. Structure and mineralogy of clay minerals. In: Bergaya, F., Lagaly, G. (Eds.), Handbook of Clay Science, 2nd ed. Elsevier, Amsterdam, pp. 21–68 (Chapter 2).
Brown, J.L., Rich, C.I., 1968. High-resolution electron microscopy of muscovite. Science 161, 1135–1137.
Bu, H., Yuan, P., Liu, H., Liu, D., Liu, J., He, H., Zhou, J., Song, H., Li, Z., 2017. Effects of complexation between organic matter (OM) and clay mineral on OM pyrolysis. Geochim. Cosmochim. Acta 212, 1–15.
Chen, T., Wang, H., 2007a. Determination of layer stacking microstructures and interlayer transition of illite polytypes by high-resolution transmission electron microscopy (HRTEM). Am. Mineral. 92, 926–932.
Chen, T., Wang, H., 2007b. Microstructure characteristics of illite from Chuanlingou Formation of Changcheng System in Jixian County, Tianjin City. Sci. China Ser. D Earth Sci. 50, 1452–1458.
Chen, T., Xu, H., Lu, A., Xu, X., Peng, S., Yue, S., 2004. Direct evidence of transformation from smectite to palygorskite: TEM investigation. Sci. China Ser. D Earth Sci. 47, 985–994.
Clinard, C., Mandalia, T., Tchoubar, D., Bergaya, F., 2003. HRTEM image filtration: nanostructural analysis of a pillared clay. Clay Clay Miner. 51, 421–429.
Drits, V.A., Guggenheim, S., Zviagina, B.B., Kogure, T., 2012. Structures of the 2: 1 layers of pyrophyllite and talc. Clay Clay Miner. 60, 574–587.
Gareth, T., Goringe, M.J., 1979. Transmission Electron Microscopy of Materials. John Wiley & Sons, New York.
Guo, H.J., Jia, W.L., Peng, P.A., Lei, Y.H., Luo, X.R., Cheng, M., Wang, X.Z., Zhang, L.X., Jiang, C.F., 2014. The composition and its impact on the methane sorption of lacustrine shales from the Upper Triassic Yanchang Formation, Ordos Basin, China. Mar. Pet. Geol. 57, 509–520.
Hong, H., Churchman, G.J., Yin, K., Li, R., Li, Z., 2014. Randomly interstratified illite–vermiculite from weathering of illite in red earth sediments in Xuancheng, southeastern China. Geoderma 214 (215), 42–49.
Iijima, S., Buseck, P.R., 1978. Experimental-study of disordered mica structures by high-resolution electron-microscopy. Acta Crystallogr. Sect. A 34, 709–719.
Jiang, W.-T., Chang, P.-H., Tsai, Y., Li, Z., 2016. Halloysite nanotubes as a carrier for the

uptake of selected pharmaceuticals. Microporous Mesoporous Mater. 220, 298–307.
Kogure, T., 2013. Electron microscopy. In: Bergaya, F., Lagaly, G. (Eds.), Handbook of Clay Science, 2nd ed. Elsevier, Amsterdam, pp. 289–294 (Chapter 2.9).
Kogure, T., Banfield, J.F., 1998. Direct identification of the six polytypes of chlorite characterized by semi-random stacking. Am. Mineral. 83, 925–930.
Kogure, T., Hybler, J., Durovic, S., 2001. A HRTEM study of cronstedtite: determination of polytypes and layer polarity in trioctahedral 1:1 phyllosilicates. Clay Clay Miner. 49, 310–317.
Kogure, T., Hybler, J., Yoshida, H., 2002. Coexistence of two polytypic groups in cronstedtite from Lostwithiel, England. Clay Clay Miner. 50, 504–513.
Kogure, T., Kameda, J., Matsui, T., Miyawaki, R., 2006. Stacking structure in disordered talc: interpretation of its X-ray diffraction pattern by using pattern simulation and high-resolution transmission electron microscopy. Am. Mineral. 91, 1363–1370.
Kogure, T., Mori, K., Kimura, Y., Takai, Y., 2011. Unraveling the stacking structure in tubular halloysite using a new TEM with computer-assisted minimal-dose system. Am. Mineral. 96, 1776–1780.
Leapman, R.D., Hunt, J.A., 1991. Comparison of detection limits for EELS and EDXS. Microsc. Microanal. Microstruct. 2, 231–244.
Liu, D., Yuan, P., Liu, H., Li, T., Tan, D., Yuan, W., He, H., 2013a. High-pressure adsorption of methane on montmorillonite, kaolinite and illite. Appl. Clay Sci. 85, 25–30.
Liu, H., Yuan, P., Qin, Z., Liu, D., Tan, D., Zhu, J., He, H., 2013b. Thermal degradation of organic matter in the interlayer clay–organic complex: a TG-FTIR study on a montmorillonite/12-aminolauric acid system. Appl. Clay Sci. 80, 398–406.
Lutterotti, L., Voltolini, M., Wenk, H.-R., Bandyopadhyay, K., Vanorio, T., 2010. Texture analysis of a turbostratically disordered Ca-montmorillonite. Am. Mineral. 95, 98–103.
Lv, G., Li, Z., Jiang, W.-T., Chang, P.-H., Liao, L., 2015. Interlayer configuration of ionic liquids in a Ca-montmorillonite as evidenced by FTIR, TG-DTG, and XRD analyses. Mater. Chem. Phys. 162, 417–424.
Marcks, C., Wachsmuth, H., Reichenbach, H.G.V., 1989. Preparation of vermiculites for HRTEM. Clay Miner. 24, 23–32.
Murakami, T., Sato, T., Inoue, A., 1999. HRTEM evidence for the process and mechanism of saponite-to-chlorite conversion through corrensite. Am. Mineral. 84, 1080–1087.
Theng, B.K.G., 2012. Formation and Properties of Clay-Polymer Complexes, 2nd ed. Elsevier, Amsterdam, pp. 201–229 (Chapter 7).
Theng, B.K.G., 2018. Clay Mineral Catalysis of Organic Reactions. CRC Press, Boca Raton, pp. 221–243 (Chapter 4).
Wenk, H.-R., 1976. Electron Microscopy in Mineralogy. Springer, New York, pp. 144–174 (Section 3).
Wu, L.M., Zhou, C.H., Keeling, J., Tong, D.S., Yu, W.H., 2012. Towards an understanding of the role of clay minerals in crude oil formation, migration and accumulation. Earth Sci. Rev. 115, 373–386.
Xi, Y., Frost, R.L., He, H., Kloprogge, T., Bostrom, T., 2005. Modification of Wyoming montmorillonite surfaces using a cationic surfactant. Langmuir 21, 8675–8680.
Yuan, P., Annabi-Bergaya, F., Tao, Q., Fan, M., Liu, Z., Zhu, J., He, H., Chen, T., 2008. A combined study by XRD, FTIR, TG and HRTEM on the structure of delaminated Fe-intercalated/pillared clay. J. Colloid Interface Sci. 324, 142–149.
Yuan, P., Liu, H., Liu, D., Tan, D., Yan, W., He, H., 2013. Role of the interlayer space of montmorillonite in hydrocarbon generation: an experimental study based on high temperature–pressure pyrolysis. Appl. Clay Sci. 75, 82–91.
Zhang, W., Kang, J.H., Lee, S.J., 2007. Visualization of saltating sand particle movement near a flat ground surface. J. Vis. 10, 39–46.
Zhang, Z., Liao, L., Xia, Z., Li, C., 2012. Montmorillonite-carbon nanocomposites with nanosheet and nanotube structure: preparation, characterization and structure evolution. Appl. Clay Sci. 55, 75–82.